GEOPHYSICS, VOL. 44, NO. 6 (JUNE 1979); P. 1116–1141, 26 FIGS., 4 TABLES.

Role of borehole geophysics in defining the physical characteristics of the Raft River geothermal reservoir, Idaho

W. Scott Keys* and James K. Sullivan*

Numerous geophysical logs have been made in three deep wells and in several intermediate depth core holes in the Raft River geothermal reservoir, Idaho. Laboratory analyses of cores from the intermediate depth holes were used to provide a qualitative and quantitative basis for a detailed interpretation of logs from the shallow part of the reservoir. A less detailed interpretation of logs from the deeper part of the reservoir is based on much less corroborative evidence. Extensive use was made of computer plotting techniques to arrive at some interpretations.

Both the stratigraphic correlation utilizing a full suite of logs and the attitude of bedding calculated from acoustic televiewer logs indicate gentle dips throughout most of the reservoir with some local flexures. Televiewer logs permitted the location and orientation of numerous fractures and several features that may be faults. Temperature and flowmeter logs provide evidence that these fractures and faults are conduits that conduct hot water to the wells.

One of the intermediate depth core holes penetrated a hydrothermally altered zone that includes several fractures producing hot water. This altered production zone could be distinguished by several logs. Borehole gamma spectrometry can be used to identify anomalous concentration of uranium, thorium, and potassium which are probably due to transportation by hydrothermal solutions. Computer crossplotting was used as an aid to the identification of such rock types as quartzite, quartz monzonite, and biotite schist in the deeper wells. Alteration of biotite schist to chlorite schist was also recognizable on these logs using computer-based analysis.

Borehole geophysics not only provided much information on the Raft River geothermal reservoir but also permitted the lateral and vertical extrapolation of core and test data and bridged the gap between surface geophysical data and core analyses.

INTRODUCTION

The southern Raft River Valley, south of Malta, Idaho, was designated a Known Geothermal Resource Area (KGRA) in 1971 by the U. S. Geological Survey (USGS) (Godwin et al, 1971) on the basis of two shallow wells that flow boiling water (Figure 1). Since then, the USGS has drilled 35 auger holes less than 30 m deep and 5 intermediate depth core holes up to 427 m deep (Crosthwaite, 1974, 1976). Also, the Idaho National Engineering Laboratory, funded by the Energy Research and Development Administration (now Department of Energy), has drilled three test wells up to 1829 m deep that may be used for production and also a shallower well that is planned for reinjection of water from the reservoir after it passes through the heat exchanger. The rocks penetrated in these holes consist of alluvium and Tertiary deposits (consisting of unconsolidated to well-consolidated sandstone, siltstone, claystone, and conglomerate, some of which are tuffaceous) to a depth greater than 1371 m. These deposits are underlain by Precambrian metasedimentary rocks, chiefly quartzite and schist, and quartz monzonite.

The study described here was carried out to develop high-temperature logging equipment and log-interpretation techniques to further the development of geothermal energy. Many types of borehole surveys were carried out using commercial logging services and two USGS research logging units. All service company logs were recorded in analog format and were later digitized under contract to the USGS. Logs made with one of the USGS logging units were recorded simultaneously in digital and analog format.

To provide background information for the lithologic interpretation of geophysical logs and to provide calibration data for quantitative log interpretation, a large number of analyses have been made of core from the shallow part of the Raft River reservoir. Few cores were obtained below 427 m. Most of the analyses of core from the intermediate depth core holes are from core hole 3 (CH-3). CH-3 (Figure 1) was selected for investigation of the shallow part of the reservoir because it was the deepest of the holes drilled by the USGS, and it encountered a flow of hot water. Core to be analyzed from the intermediate depth holes was selected largely on the basis of log response. Core analyses were obtained from three sources: the majority were done by the hydrologic laboratory of the USGS; radiometric analyses for uranium, thorium, and potassium were performed by the Isotope Geology Branch of the USGS; and Core Laboratories, Inc. measured acoustic velocity,

Manuscript received by the Editor August 14, 1978; revised manuscript received December 6, 1978.
*U.S. Geological Survey, WRD, M.S. 403, Box 25046, Denver Federal Center, Denver, CO 80225.
0016-8033/79/0601—1116$03.00. This paper was prepared by an agency of the U.S. government.

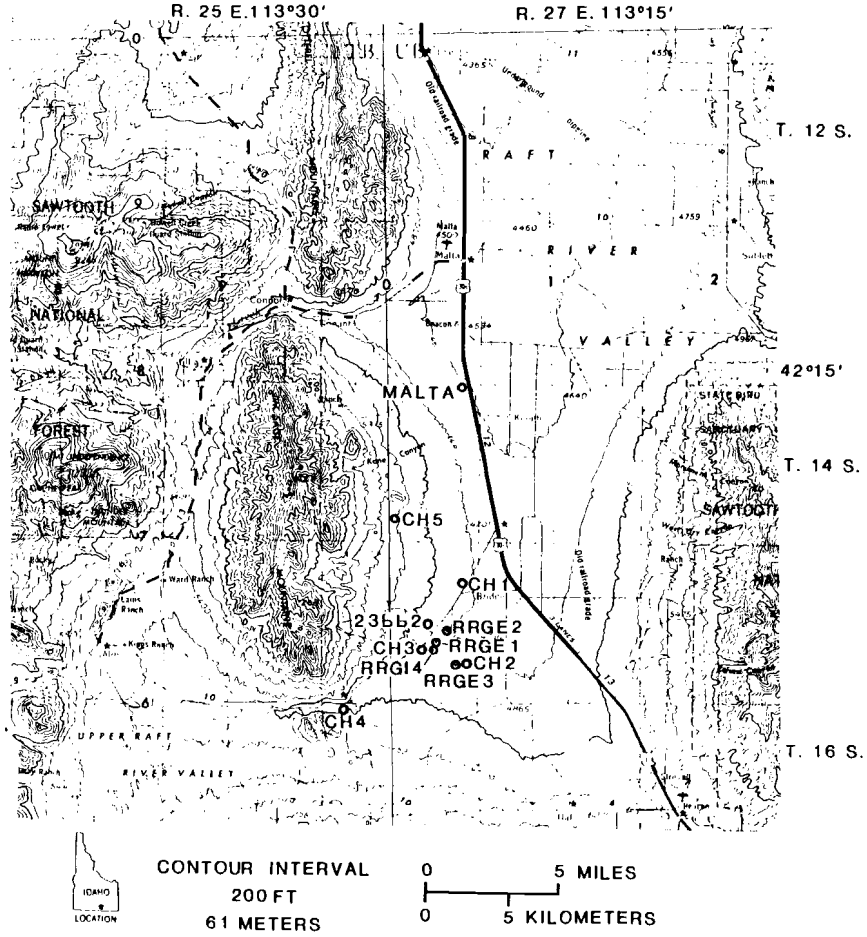

FIG. 1. Topographic map showing location of most important core holes and wells, Raft River Project.

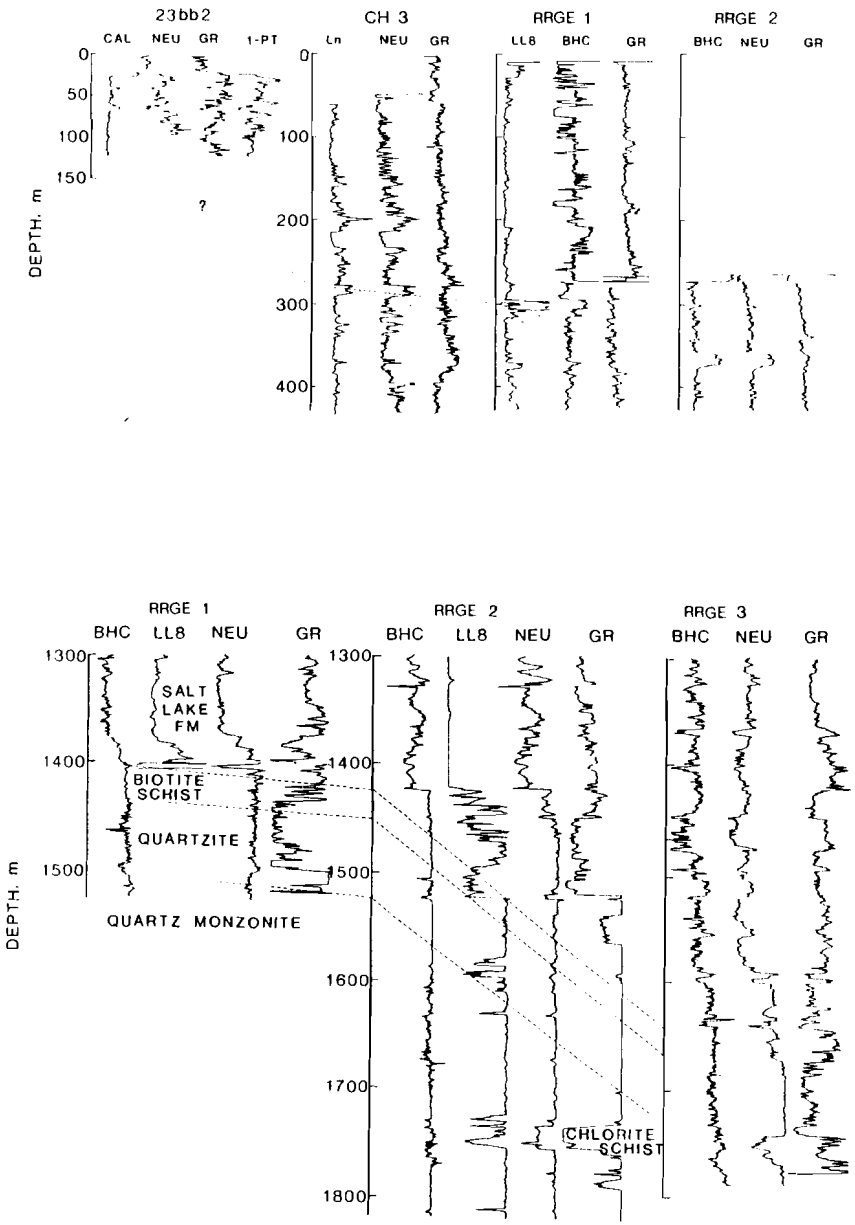

FIG. 2. Two cross-sections of Raft River holes; correlation is based on logs identified as caliper (CAL), neutron (NEU), gamma-ray (GR), single-point resistance (1-PT), long normal resistivity (LN), Laterolog-8 (LL8), and acoustic velocity (BHC).

porosity, formation resistivity factor, grain-size distribution, and permeability on a small number of samples.

The hydrologic laboratory of the USGS has completed a number of analyses; namely, lithologic description; x-ray mineralogic analyses for quartz, potassium feldspar, plagioclase feldspar, calcite, dolomite, analcime, stilbite, cristobalite, and clay; porosity, total, and effective; pore-size distribution; grain and bulk density; permeability to liquid; and grain-size distribution and $CaCO_3$ content.

Crossplotting of data from two logs and the available core data in the computer was the most important technique used for analysis of the Raft River logs. In crossplotting, the values from one log are plotted against values from another log at corresponding depths. The crossplots were all made on a CRT (cathode-ray-tube) computer-graphics terminal so that the depth sequence of pattern development could be observed as the plot was being generated. The program made depth information and selectable depth intervals available to the log analyst while crossplots were being generated, so that depth intervals represented by distinct patterns on the crossplots could be identified.

RESERVOIR PROPERTIES

Stratigraphic correlation

Stratigraphic correlation was attempted only for the holes near the Raft River geothermal wells (from CH-1 on the north to RRGE-3 on the south, inclusive, shown in Figure 1). The stratigraphic correlation illustrated in Figure 2 used only geophysical well logs. It was subsequently checked against correlations made on the basis of well cuttings and core, and the two are in substantial agreement. Correlation in the Precambrian schist, quartzite, and quartz monzonite was rather straightforward. Correlation in the overlying sedimentary and volcanic rocks (Tertiary Salt Lake formation and the Pleistocene Raft formation) was quite difficult and much less certain because of their lenticular nature, the presence of hydrothermal alteration, and the poor quality logs obtained in the large-diameter intervals of the RRGE wells. The altered zone in CH-3 is characterized by a significant increase in analcime and quartz and a decrease in plagioclase and potassium feldspars. This zone, which contributes most of the hot water to this well, was not recognized in the core log, nor is it clearly defined on most geophysical logs. Varying degrees of alteration and changes in the thickness of altered zones can complicate the procedure of determining stratigraphic equivalence from logs.

Correlation was also made more difficult by differences between log response and the variety of logs run by different organizations. The same complete suite of logs was not available for each well. The very large diameter in intervals of RRGE-1 was the cause of some rather poor logs. When a tentative stratigraphic correlation was made with one type of log, substantiation was attempted with other types. Logs

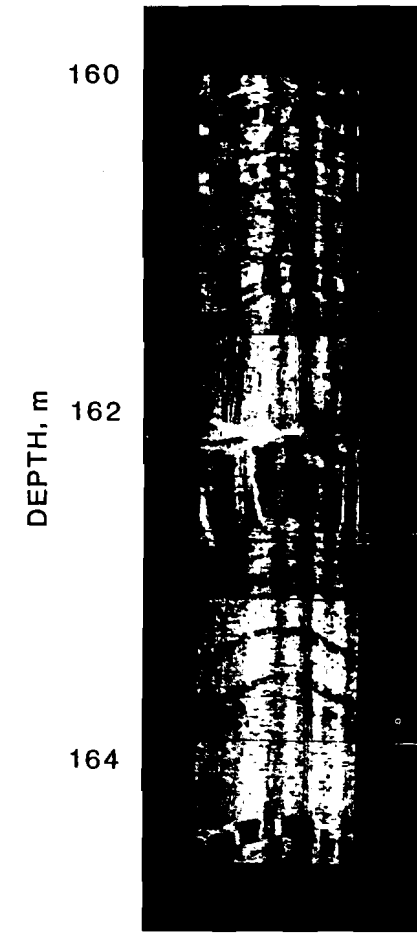

FIG. 3. Acoustic televiewer log from 160 to 164.6 m, CH-3. Bed dips 45 to 55 degrees in the direction N30°–40°E.

used for correlation in estimated order of utility are (1) various types of resistivity logs, (2) natural gamma, (3) neutron, (4) acoustic velocity, and (5) caliper. There were too few core analyses to provide any basis for correlation.

Log correlations indicate that the structure penetrated by the holes drilled at Raft River to date is rather simple, and dips are not very steep over large areas. In contrast, the acoustic televiewer logs show dips of bedding as high as 45 to 55 degrees, and measured dips on cores are as high as 20 to 30 degrees (Covington, 1974, written communication). Figure 3 is an interval of the acoustic televiewer log of CH-3 showing very clearly defined bedding that has a consistent dip of 45 to 55 degrees. The direction of dip apparently averages N30°–40°E, but may be in error because of possible equipment malfunctions. It is doubtful if a significant part of either of these measurements is due to hole deviation; it is more likely that the steep dips represent local flexures or possibly tilting of blocks caused by faulting. If the correlations shown on Figure 2 are correct, the dip of a bed can be calculated from the depth at which it intersects three holes. One bed can be seen on the neutron (NEU) and acoustic (BHC) logs at 85 m in 23bb2, at 280.4 m in CH-3, and at 295.3 m in RRGE-1, which gives a dip of 14 degrees and strike of S41°E. The base of the Tertiary is at 1402 m in RRGE-1, at 1419 m in RRGE-2, and at 1643 m in RRGE-3. These points give a dip of 7 degrees and a strike of S53°E if there are no faults between the wells. Because of local structures, the dips calculated from correlations may not be meaningful.

Injection well RRGI-4 is approximately 549 m south of RRGE-1 and the collar elevation is 12 m lower than CH-3. Although there are significant differences in the logs, a fairly reliable correlation was made between RRGI-4 and CH-3. Correlative lithologic units are approximately 61 m deeper in RRGI-4 than in CH-3. Added to the difference in elevation between the wells, this signifies either a steeper than normal dip or offset along a fault between the two wells. The televiewer log of RRGI-4 is of poor quality, but the beds that are discernible appear to be nearly horizontal.

Malta well.—A complete suite of logs was not made on the Malta well because the weight-bearing structure at the well head was considered inadequate. The logs that were made reached maximum depths of from 1494 to 1524 m where the well is bridged. The total depth drilled is reported as 2069 m. The lack of anomalies on the temperature log suggests that most of the hot water that flows when the well is opened enters from below the maximum depth logged, apparently through the bridge. The maximum in-hole temperature recorded was 92.38°C and the minimum was 42.28°C. Because facilities were not available to store or dispose of the large volume of water produced, it was not possible to log with the well flowing.

Based on the gamma log, a very tentative correlation can be made with a lithologic unit having higher than average radioactivity in RRGE-2. The unit correlated is at a depth of approximately 910 m in the Malta well and approximately 1190 m in RRGE-2. The thickness of this unit, as defined in the description of cuttings from the Malta well, does not agree with the interpretation of the gamma (GR) log, but it is described as a silty-to-sandy claystone which is usually more radioactive than coarser-grained sediments. The typical relationship of radioactivity and grain size may not hold true at Raft River where there are nearby sources of silicic volcanic and granitic detritus.

Several of the logs suggest a major change in lithology at a depth of approximately 1020 m. The rocks above this depth have a very low resistivity and are less radioactive (except for the unit at 910 m). The caliper log indicates that, for the most part, the rocks above 1020 m are represented by a wider range of lithology and are not as well cemented as the underlying rocks. The description of the cuttings by Oriel and Williams (1975) of the USGS indicates a contact at 997 m between tuffaceous sediments above and mostly altered tuffs below. The alteration minerals are reported to include zeolites, quartz, and chalcedony which could account for the apparent increase in cementation. None of the logs provides a basis for recognizing the rhyolite and volcanic glass reported in the cuttings; however, a change to less altered rocks below 1378 m is clearly defined on the logs.

Table 1. Upper and lower contacts inferred from core analysis.

	Potassium feldspar	Plagioclase feldspar	Quartz	Analcime
Upper contact, depth (m)	302	302	326	302 or 326
Lower contact, depth (m)	354	381	360	354

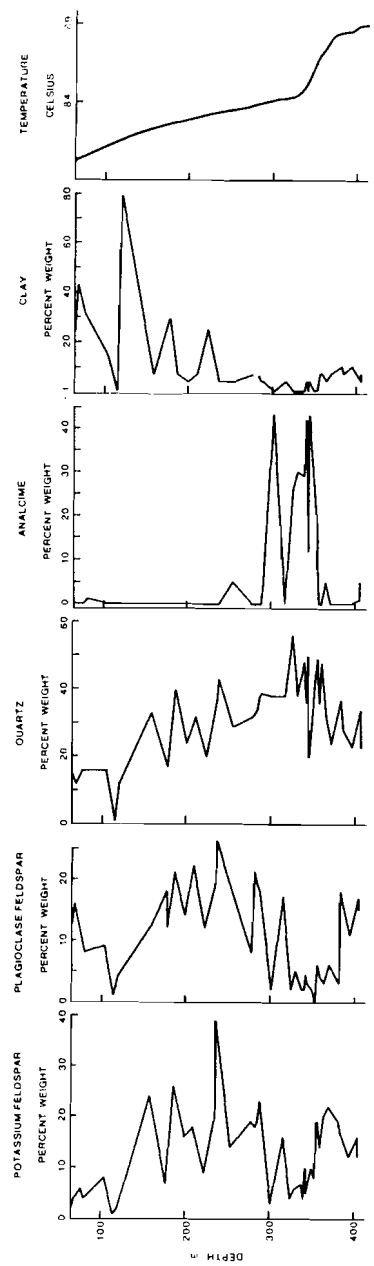

FIG. 4. Computer plots of potassium feldspar, plagioclase feldspar, quartz, analcime, and clay percentages determined by x-ray diffraction techniques on core from CH-3 along with a temperature log.

Lithology

Hydrothermal alterations.—Information from logs or core on the location and kind of hydrothermal alteration is important in locating present and past zones of hot water movement. The only specific data available on hydrothermal alteration in the shallow part of the reservoir were obtained from core analyses, chiefly x-ray diffraction mineralogy from samples taken from CH-3 which is only 427 m deep. Figure 4 is a composite plot of potassium feldspar, plagioclase feldspar, quartz, analcime, and clay determined by x-ray analysis of core with a temperature log to provide data on hot water entry. The main zones of hot water entry are at depths from 346.9 to 347.5 m and from 336.8 to 337.1 m as defined by logs. The analyses shown in Figure 4 suggest a thick zone depleted in feldspar and enriched in quartz and analcime that extends above and below the main depths of present water movement. The upper and lower contacts of the zone of alteration inferred from core analyses are given in Table 1.

The intervals depleted in feldspars and enriched in analcime are quite clearly defined. The zone enriched in quartz is poorly defined, but a statistical analysis suggests that a meaningful change occurs in the zone from approximately 325 to 360 m as shown in Table 2. The correlation coefficient between the analcime and potassium feldspar percentages (Figure 4) for the interval of interest, 326–360 m, is −0.90 and the covariance is −66.04 and −60.53. Although this excellent negative correlation would suggest that analcime is derived from potassium feldspar, mineralogical considerations indicate it must actually be derived from plagioclase feldspar. The correlation coefficient for analcime and plagioclase feldspar is not nearly so high, and Figure 4 shows that the bottoms of the zones do not coincide. Apparently leaching and upward movement of sodium aluminum silicate have taken place. Several researchers have reported on the occurrence and metastable relationship of albite and analcime (Coombs et al, 1959; Campbell and Fyfe, 1965). Campbell and Fyfe (1965) suggest that the reaction analcime and quartz = albite + liquid water is in equilibrium at 190°C or possibly lower temperatures. Salinity, silica species, solid solutions in feldspars, and other factors may influence equilibria, but the data do suggest higher temperatures at one time in this depth interval (326–360 m). If a geothermal gradient of 20°C/km is assumed, the analcime reaction which takes place at a temperature of 150°C would occur at a depth of 7.0 km. At shallower depths and therefore lower

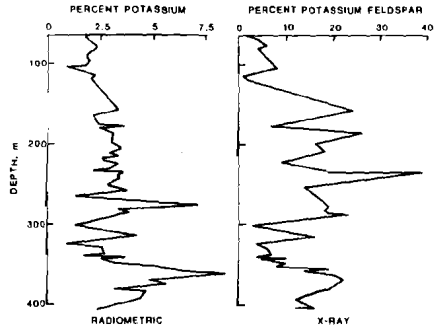

FIG. 5. Computer plots of potassium-40 percentage from radiometric analyses and potassium feldspar percentage derived from x-ray analyses of samples from CH-3.

pressure, higher temperatures would be required if all other factors were the same.

Can geophysical well logs be used to locate or define altered zones in the Raft River region? An obvious candidate is the in-hole measurement of gamma spectral data, which are discussed under distribution of radioisotopes. Potassium-40, determined by radiometric or in-hole spectral analysis, should relate to the content of potassium feldspars if other potassium-rich minerals are not abundant. Figure 5 shows the relationship between potassium-40 and potassium feldspar percentages as determined from core analyses. The correlation coefficient is only 0.50 when all of the data are considered but is 0.86 when only the data from the altered zone from 326–360 m are analzyed. The use of gamma spectrometry to identify intervals with low potassium content may not uniquely distinguish altered zones because potassium content is also low above 122 m in CH-3. Another log which may help identify altered zones is that of acoustic velocity. Both in-hole and core measurements indicate that acoustic velocities are higher in the altered zone than in overlying and, probably, underlying rocks. More core data from deeper holes are needed for confirmation, however.

All of the core data and logs from CH-3 suggest that the hole penetrated a zone of hot water production where significant hydrothermal alteration has taken place. This altered zone in CH-3 apparently does have a lower boundary of water flow, which suggests that at this location the movement of hot water has an important lateral as well as vertical component.

A petrographic study of the andesite porphyry in CH-4 revealed significant hydrothermal alteration. Large open fractures in this porphyry are transmitting hot water. Smaller fractures seen in thin sections are filled or lined with iron oxides, pyrite, feldspar crystals, cristobalite, and chalcedony. The groundmass shows reorganization of silica to chalcedony and feldspar to clay. Chloritization, which has taken place in schists penetrated in RRGE-2, is also prevalent in the andesite in CH-4. Chlorite content appears to increase with depth.

Hydrothermal alteration is extensive in the deeper part of the Raft River reservoir, but data on its character are scarce. There is an interval of biotite schist, approximately 30 m in thickness, present between the Precambrian quartzite and the overlying Salt Lake formation in all three RRGE wells. It is characterized by increased radiation recorded on the gamma log and a somewhat higher apparent porosity on the neutron log. In contrast, RRGE-2 was drilled sufficiently deep to intersect an interval of schist within the quartz monzonite that exhibits a remarkably different response on these two logs (Figure 6). In the depth interval from 1734 to 1756 m, there is low intensity on the gamma log, a high apparent neutron porosity, and a high bulk density. The average deflection on a commercial gamma log in this interval is between 25 and 50 American Petroleum Institute (API) units, which is less than any other interval in the well and significantly less than the quartz monzonite, which exceeds 340 API units. The commercial gamma log did not respond to higher radiation intensities in the quartz monzonite, but the USGS gamma log shows that considerable variation exists in this rock. In the altered zone, 1734–1756 m, the neutron log indicates a higher apparent porosity than any of the rocks below 1280 m and the gamma-gamma log indicates the highest bulk density in the well, ranging from 2.9 to 3.0 g/cm^3. All of the caliper logs indicate that the altered zone is penetrated by a hole of uniform diameter. Therefore, none of the log response described

Table 2. Quartz contents from core analysis.

Depth interval (m)	Number of samples	Quartz (percent) Mean	Quartz (percent) Standard deviation
63.7–198.7	12	18.50	10.18
209.4–315.8	11	34.55	6.23
324.9–359.7	11	42.00	9.91
364.0–412.7	8	30.25	6.84

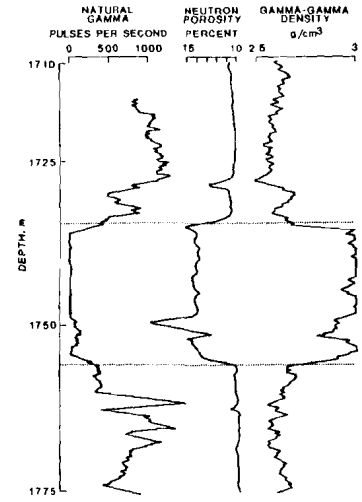

FIG. 6. Gamma log, neutron log, and gamma-gamma log for the depth interval 1710–1775 m in RRGE-2.

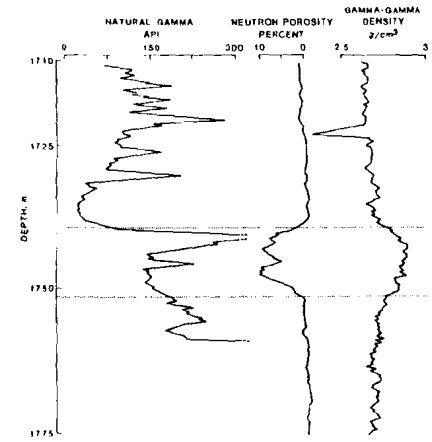

FIG. 7. Gamma log, neutron log, and gamma-gamma log for the depth interval 1710–1775 m in RRGE-3 leg 3C. The neutron log is scaled in American Petroleum Institute (API neutron units).

is due to hole-diameter effect. Figure 7 illustrates the response of the same three logs in leg C of RRGE-3. Leg C is the third directionally drilled borehole (leg) from within RRGE-3. The response indicates that the lithology from a depth of 1739 to 1752 m is biotite schist rather than chlorite schist.

Neither the acoustic velocity nor the deep induction logs of RRGE-2 demonstrate a unique response in the altered rocks. The deep induction log is offscale through most of the interval, except for a decrease below 80 Ω-m from 1747 to 1750.5 m where the gamma log is highest for the altered zone. The Laterolog-8 shows that part of the altered zone has a lower resistivity than the adjacent adamellite. The USGS 16- and 64-inch normal curves clearly delineate the altered zone as having a lower resistivity than adjacent rocks.

The cuttings from RRGE-2 for the depth interval 1734 to 1756 m were logged as a chlorite schist. The rest of the interval from about 1524 m to a total depth of 2012 m is described as adamellite, which is a variety of quartz monzonite containing nearly equal proportions of plagioclase and orthoclase feldspar. The adamellite averages about 10 percent biotite and chlorite, with some zones as high as 25 percent. Both cuttings and logs suggest that the altered zone has the highest percentage of chlorite or biotite and the most complete alteration from biotite to chlorite of any rock penetrated by the hole. The chlorite schist has a low gamma response due to the removal of potassium during alteration from biotite to chlorite. Leaching of uranium and thorium may also have taken place, but no gamma spectral data are available to substantiate this hypothesis. The neutron log shows an apparent high porosity (12 percent average) because the probe responds to bound water the same as to water in pore spaces. The high bulk density shown on the gamma-gamma log is due in part to the high density of chlorite, approximately 2.9 g/cm^3. Log inaccuracy or inclusions of heavy minerals may account for the average 2.9–3.0 g/cm^3 recorded.

Crossplots of various logs have been used in an attempt to characterize response to the rock types present in the deeper part of RRGE-2 and to develop predictive techniques. The procedure was to develop a crossplot for the depth interval 1286 to 1826 m on the CRT computer-graphics terminal and then select smaller depth intervals for plotting, as described previously. Crossplots of gamma-gamma, neutron, sonic, and induction logs were made for this depth interval. An M–N plot was also generated as described by Burke et al (1979). Variables M and N are calculated from acoustic velocity, density, and neutron log response to the rock and to its contained

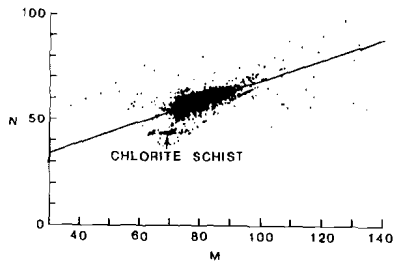

FIG. 8. M–N computer plot for the depth interval 1286–1825 m, RRGE-2.

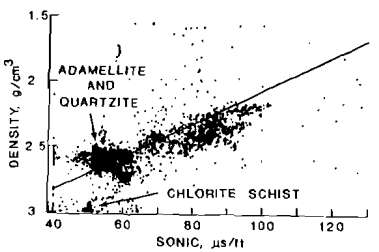

FIG. 9. Computer-generated crossplot of sonic log and gamma-gamma density log values for depth interval 1286–1825 m, RRGE-2.

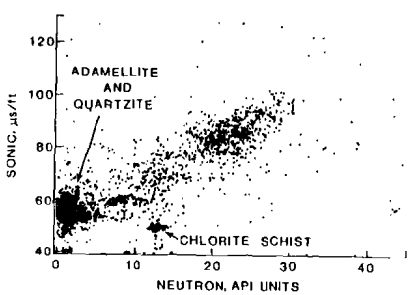

FIG. 10. Computer-generated crossplot of neutron log and sonic log values for depth interval 1286–1825 m, RRGE-2.

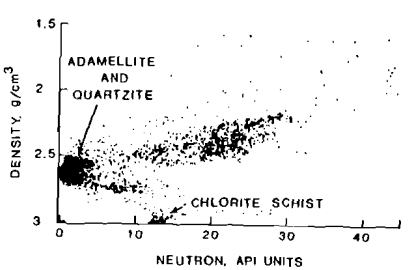

FIG. 11. Computer-generated crossplot of neutron log and gamma-gamma log values for depth interval 1286–1825 m, RRGE-2.

fluids. M and N are essentially independent of primary porosity and dependent on lithology. The M–N plot clearly distinguished the chlorite schist (Figure 8).

The crossplots of gamma-gamma (density), neutron, and sonic logs show the altered zone from 1734 to 1756 m as a distinct and separate cluster of points (Figures 9, 10, and 11). Plotting by depth interval proved that only the altered zone contributes points to the cluster and that all of the digitized points in the altered zone fall within the cluster. The altered zone cluster has an average transit time of 50 μsec/ft, an average neutron porosity of 12.5 percent, and an average bulk density from gamma-gamma logs of 3.0 g/cm^3. This last value may be slightly low because the commercial log was set to limit at 3.0 g/cm^3. Crossplots of induction resistivity versus other log parameters are not included here because the log response was limited at about 1700 Ω-m due to tool design.

Figures 9, 10, and 11 also show a major cluster of points that represent the adamellite and quartzite. The average log values for this cluster are: transit time, 50–60 μsec/ft; neutron porosity, 0–4 percent; and bulk density, 2.5–2.7 g/cm^3. These are reasonable values for adamellite and quartzite. The quartzite is clearly distinguished from the adamellite by its lower gamma radiation and lower resistivity on the normal and Laterlog-8 resistivity curves. The elongate group of points trending toward longer transit time, higher porosity, and lower bulk density represents the overlying sediments of the Salt Lake formation which may be altered.

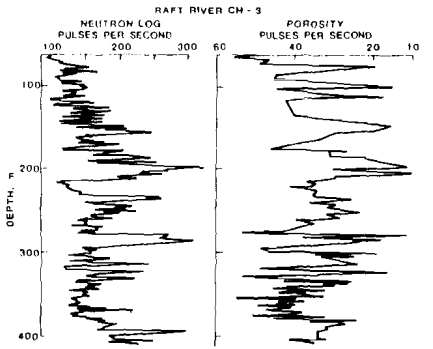

FIG. 12. Neutron log and laboratory analyses for total porosity from CH-3 core samples.

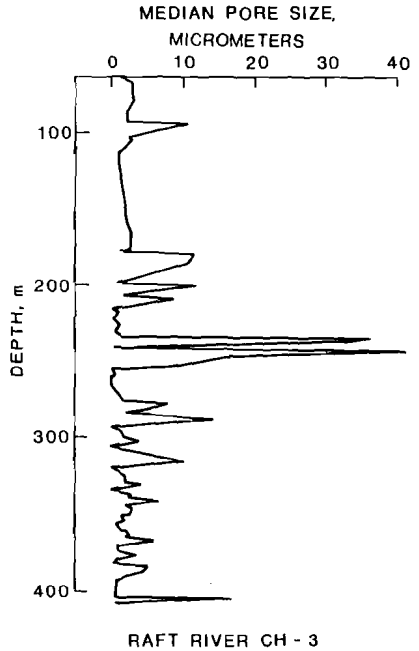

FIG. 13. Median pore size as a function of depth, CH-3.

Porosity.—The porosity of the reservoir rocks at Raft River is an important parameter because of its relation to the amount of water in storage. A large number of analyses for total and effective porosity have been made of core from the Raft River, and these data are summarized in Table 3. Total porosity includes pore spaces, whether interconnected or not. Effective porosity includes only those pore spaces that are connected in such a way that water can be transmitted. There is a rather small and consistent difference between total and effective porosity in CH-3; total porosity averages 3.5 percent higher than does effective porosity. The character of the neutron, acoustic velocity, and gamma-gamma logs is more closely related to total porosity than to effective porosity. The various kinds of resistivity logs are more closely related to effective porosity, but the conductivity of the fluid in the connected pore spaces also has a major effect on the response of these logs.

Figure 12 shows the general relationship between an uncalibrated, noncompensated neutron log in CH-3 and total porosity from CH-3 core analyses. It can be seen that the major changes in porosity were recorded on the neutron log, but there are significant differences between the two sets of measurements. Porosity values scaled from commercial porosity logs of other holes are highly erratic and inconsistent with the core analyses available for CH-3. These logs, of course, were obtained using equipment and interpretive procedures developed for oil field conditions, without benefit of local core analyses. The important point is that core analyses are necessary in order to substantitate quantitative interpretation of any logs in a novel environment.

If a consistent relationship exists between formation resistivity factor (F) and porosity (ϕ) for these rocks, then data from porosity and resistivity logs can be used to calculate water quality (Keys and MacCary, 1971).

The formation factor can be calculated from an estimate of porosity from a log such as acoustic velocity, neutron, or gamma-gamma and an estimate of cementation factor from laboratory measurements. The resistivity of the rocks 100 percent saturated with water (Ro) can be derived from multiple electrode resistivity logs to enable calculation of Rw, the resistivity of the formation water.

Although the number of samples was smaller than one might desire, the correlation coefficient calculated for ϕ and F measured on 13 core samples from CH-3 is -0.80 at zero overburden pressure. At an effective overburden pressure of 550 psi, the correlation coefficient is -0.85. The cementation factor is 1.82

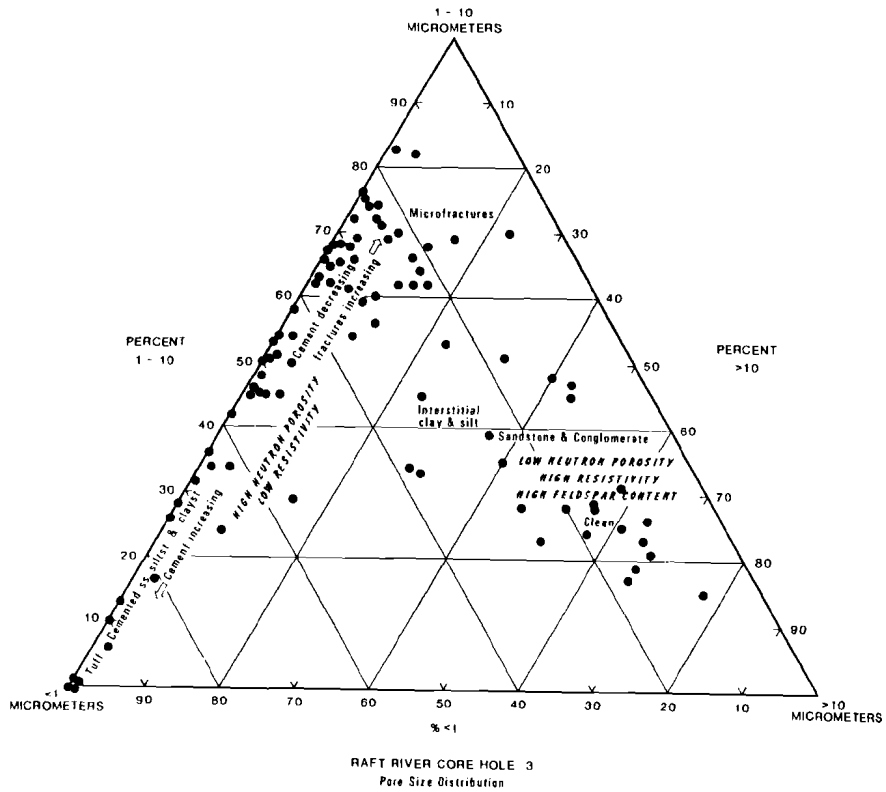

FIG. 14. Three-component diagram of pore size distribution, CH-3.

Table 3. Summary of laboratory analyses for porosity (ϕ), formation factor (F), and acoustic velocity ($\Delta\tau$).

Core hole (1)	No. of samples (N) (2)	Mean effective ϕ and standard deviations (3)	Mean F and S (4)	Correlation coefficient column (3)–(4) (5)
CH-1	10 (F = 6)	36.31 (S = 10.79)	2.77 (S = 1.12)	—
CH-2	4 (F = 2)	33.20 (S = 2.38)	5.68 (S = 4.03)	—
CH-5	3 (F = 2)	14.43 (S = 10.38)	52.85 (S = 20.72)	—
CH-3*	13	29.16 (S = 9.13)	14.13 (S = 14.04) mean total ϕ	−0.80
CH-3*	90	31.55 (S = 1.19)	35.01 (S = 10.27) mean $\Delta\tau$ (μsec/ft)	0.90
CH-3*	30	35.58 (S = 9.68)	155.77 (S = 28.18)	0.87

*Three different sets of samples from CH-3 were analyzed, each by a different laboratory. Total ϕ and $\Delta\tau$ were measured respectively by each of two laboratories instead of F.

at zero pressure and 1.99 at an effective overburden pressure of 3,800,000 N/m² (550 psi). This is approximately equivalent to the overburden pressure at half the depth of the hole.

Because of temperature problems with equipment, we did not obtain a continuous acoustic-velocity log of CH-3, but we were able to make a number of stationary measurements in the hole. The correlation coefficient for porosity and acoustic transit time measured on the core is 0.87. Thus, it appears that acoustic-velocity logs could be used to estimate porosity in this hole.

Data from pore-size distribution studies not only provide some of the same relationships to lithology as grain-size distribution, but pore size has a more direct bearing on the ability of rocks to transmit fluids. A few grain-size distributions measured on Raft River cores show good correlation with pore-size distribution. Pore-size distribution was measured by the mercury-injection method. Figure 13, a depth plot of median pore size, clearly distinguishes the sandstone at 244 m and several of the conglomerates and siltstones.

The mean of the median pore size for CH-3 is 4.72 μ (microns), but the distribution is skewed. Several studies suggest that when pore sizes greater than 2.9 μ occur in sedimentary rocks, they will readily yield cold water by means of gravity drainage.

A three-component diagram (Figure 14) shows pore-size distribution for CH-3. The pore-size ranges shown are less than 1 μ, 1–10 μ, and greater than 10 μ, respectively. All samples in the center and lower right, which indicate higher percentages of pore diameters greater than 10 μ, are sandstone and conglomerate. The amount of interstitial clay and silt reported in these samples increases toward the left. The samples showing a large percentage of pores less than 1 μ are tuff, claystone, and siltstone. The degree of cementation in these samples seems to increase from the top of the plot (1–10 μ) to the left (<1 μ). Conversely, the number of small fractures, both filled and open, reported in the samples increases from lower left toward the top; this leads to the surprising conclusion that the intergranular pore sizes in the sandstone and conglomerates are larger on the average than the microfractures. This relationship may also indicate that the finer-grained sediments or tuffs were preferentially fractured. There is some corroborating evidence from acoustic televiewer logs that the larger fractures are more prevalent in harder, more cemented rocks.

No significant relationship has been found between pore-size distribution and intrinsic permeability measured on cores. There is an apparent correlation between total porosity and the percentage of pores less than 1 μ in size. This does suggest that total porosity, however derived, might not be the best measure of the ability of shallow reservoir rocks at Raft River to store or release water.

Some of the geophysical logs made in CH-3 do have an apparent relationship to pore-size distribution (Figure 15). The highest apparent neutron porosities correspond to those intervals with the highest percentages of small pore sizes which are clays, silts, and tuffs. Conversely, the lowest apparent neutron porosities are in the intervals with the larger pores which contain sandstones and conglomerates. The correlation of absolute values between log and core

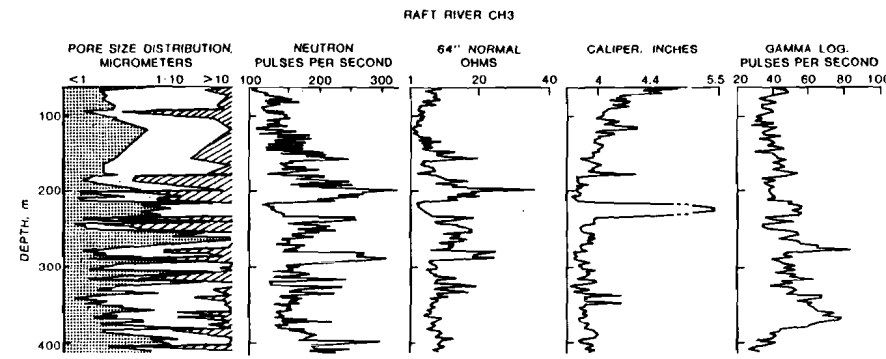

FIG. 15. Pore-size distribution, neutron, 64-inch nominal resistivity, caliper and gamma logs, CH-3.

analyses is not good; however, the neutron log does serve to identify the major lithologic units distinguished by very large or very small average pore size. The resistivity log shows a positive correlation with the larger pore sizes and a negative correlation with the smaller pore sizes; that is, the highest resistivities correlate with the presence of sandstones and conglomerates and the lowest resistivities correlate with tuffs, clays, and silts.

The natural gamma log shows a fair correlation with pore-size distribution except for the altered zone. Above the altered zone, sediments with the smallest pores are the most radioactive.

Among the minerals determined by x-ray analysis, only potassium and plagioclase feldspar show a good positive correlation with an increase in pore size. This may indicate that the sandstones and conglomerates are arkosic.

The effect of hydrothermal alteration on pore-size distribution, and thus on the ability of these rocks to transmit water, has an important bearing on reservoir evaluation. The content of analcime, which is the most positive indicator of hydrothermal alteration, is higher in the intervals with a greater percentage of pores with sizes from 1 to 10 μ and few pores larger than 10 μ. Only one of the samples taken from the altered zone has more than 75 percent pores with size less than 1 μ, and only one such sample falls in the group of sandstones and conglomerates with large pores (Figure 14). Most of the samples from the altered zone lie in the group with 60 to 80 percent pores with sizes from 1 to 10 μ. Lithologic descriptions of this group of samples by the USGS hydrologic laboratory indicate an abundance of microfractures. These microfractures and major fractures, detected by the televiewer, may have made these rocks more permeable to altering fluids. Thus, we have no direct evidence that pore structure has been changed by hydrothermal alteration; however, there is some evidence that abundant microfractures may have allowed alteration to proceed.

Permeability.—Fluid permeability is the most important parameter related to the ability of an aquifer to produce water. Unfortunately, no geophysical log is related directly to permeability. Twenty-eight measurements of the intrinsic permeability of core from the intermediate depth holes were made. The results varied over a range of seven orders of magnitude with the lowest values of 10^{-4} mD in adamellite from CH-5, and the highest of 740 mD in sandstone from CH-3. The permeabilities measured on many of these cores are suspect because the interstitial clay swelled when it came in contact with simulated formation water. No meaningful relationship was found between any logs or other core measurements from the shallow holes and intrinsic permeabilities measured on core. However, the acoustic televiewer, caliper, temperature, and flowmeter logs do provide data on the location and relative magnitude of the more permeable zones. Not enough data are available to warrant a discussion of permeability in the deep RRGE wells. Computer-derived permeabilities are discussed in the section on log interpretation.

Sources of hot water

Flowmeter and temperature data.—RRGE-2 is the only well where a comprehensive study of flowmeter and temperature data was undertaken by the USGS. Two temperature logs were used for this analysis. One was made with the tool moving up while the well was flowing. A number of flowmeter logs were also made with an impeller flowmeter while the well was producing. RRGE-2 had a complex history which makes the interpretation of temperature logs particularly difficult. The well was originally drilled to a depth of 1829 m and produced a large volume of hot water, part of which was reinjected at lower temperatures. It was then deepened to 1981 m in March 1976, and more hot water was produced. The logs described herein were recorded shortly after the well was deepened.

The following equations were used to calculate the computer flow logs which were computer plotted

$$Q_{tot} = [v_l + Q_{fa}/\pi\rho^2]\pi R^2, \quad (1)$$

and

$$Q_{fa}/\pi\rho^2 = kp, \quad (2)$$

where

Q_{tot} = total volume rate of flow,
Q_{fa} = volume rate of flow through flowmeter,
ρ = radius of flowmeter,
R = radius of hole,
p = pulse rate,
k = a conversion factor, and
$v_l = \mathbf{v} \cdot \hat{\mathbf{u}}_l$,

where $\mathbf{v}$ = velocity of the flowmeter and $\hat{\mathbf{u}}_l$ = a unit vector in the direction of flow.

At each of four depth intervals, the flowmeter was run up and down a short section of hole at various logging speeds. The data were plotted as logging speed v_l versus impeller count rate p (Figure 16).

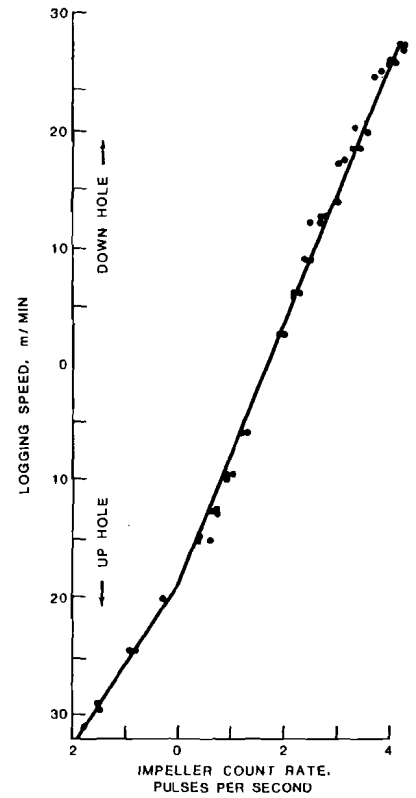

FIG. 16. Flowmeter plot for a cased section of RRGE-2.

The data plotted in Figure 16 were recorded in casing where long depth intervals of 279-mm constant casing diameter, known circular shape, and low turbulence were available. The data points are well fitted by two straight lines having different slopes, which represent the two directions of impeller rotation.

The point at which these two lines intersect represents zero Q_{fa}. The range of tool speeds around this point is the stall zone, where Q_{fa} is too small to keep the impeller rotating. The multiple-pass data points recorded at a depth of 1826 m, which is in an uncased part of the hole, were somewhat scattered and were too few to fit a curve, but the borehole diameter was very nearly the same as for the data of Figure 16. Therefore, two straight lines were imposed using the values of k derived from Figure 16. Both lines intersect the logging speed axis at the origin, giving a clear indication that the volume of flow at this depth is nearly zero.

The k values derived from Figure 16 are not appropriate for the other two sets of multiple-pass flow data, where the hole was a different diameter. Imposing straight lines with those k values gives two different intercepts on the logging speed axis. One intercept indicates upflow and the other shows downflow. Therefore, k values derived from Figure 16 cannot be applied quantitatively at other borehole diameters, and k is at least a function of borehole size. In the absence of quantitative information on the functional dependence of k on borehole size, the computed logs are presented in arbitrary units of volume rate of flow.

Under flowing conditions there is no indication of significant production below a depth of 1811 m in RRGE-2. A similar conclusion was reached by Kunze et al (1977). The abrupt change of 3.2°C at 1899 m on the shut-in temperature log, which increased to 3.9°C on the temperature log recorded when the well was flowing at the surface, is not an indication of in-flow (Figure 17); the change is too small under different flow conditions, and the flow logs show no overall change in flow rate. The changes in computed flow at 1829 m are a consequence of the method of approximation of the constant k (Figure 17).

The multipass crossplot at 1826 m indicates negligible flow. At 1811 m the temperature logs indicate some in-flow, but it is too small to register on the computed flow logs. The shut-in temperature log exhibits a thermal low at 1811 m. At the same depth, the temperature log made with the well flowing shows an inflection. A zone of colder fluid causes a temperature minimum when not flowing, but when allowed to flow up-hole, the cold fluid depresses the temperature at a depth interval above the depth of the source zone. This cold fluid can be assumed to be part of the 40 million liters (L) of cold (43°C) fluid injected prior to deepening the hole from 1829 to 1981 m (Sandquist et al, 1976).

One set of equations relating inflow volume and temperature can be found in the complex model for calculating the temperature of inflows, which is presented by Sandquist et al (1976). Their model requires input of the temperature in the borehole, the exact volume of flow at the inflow depth, and the tempera-

ture and volume of flow at a depth below the inflow. We have already demonstrated that accurate measurements of volume of flow in RRGE-2 are difficult to obtain. For this reason a simpler model is presented here.

The change of heat energy is related to temperature change by

$$\Delta q_i = m_i c_i (\Delta t_i), \quad (3)$$

where Δq_i is the change in heat energy, c_i is heat capacity, m_i is mass, and Δt_i is temperature change of fluid i. If two fluids mix adiabatically, the total change in heat energy is zero, or

$$\Delta q_i = 0. \quad (4)$$

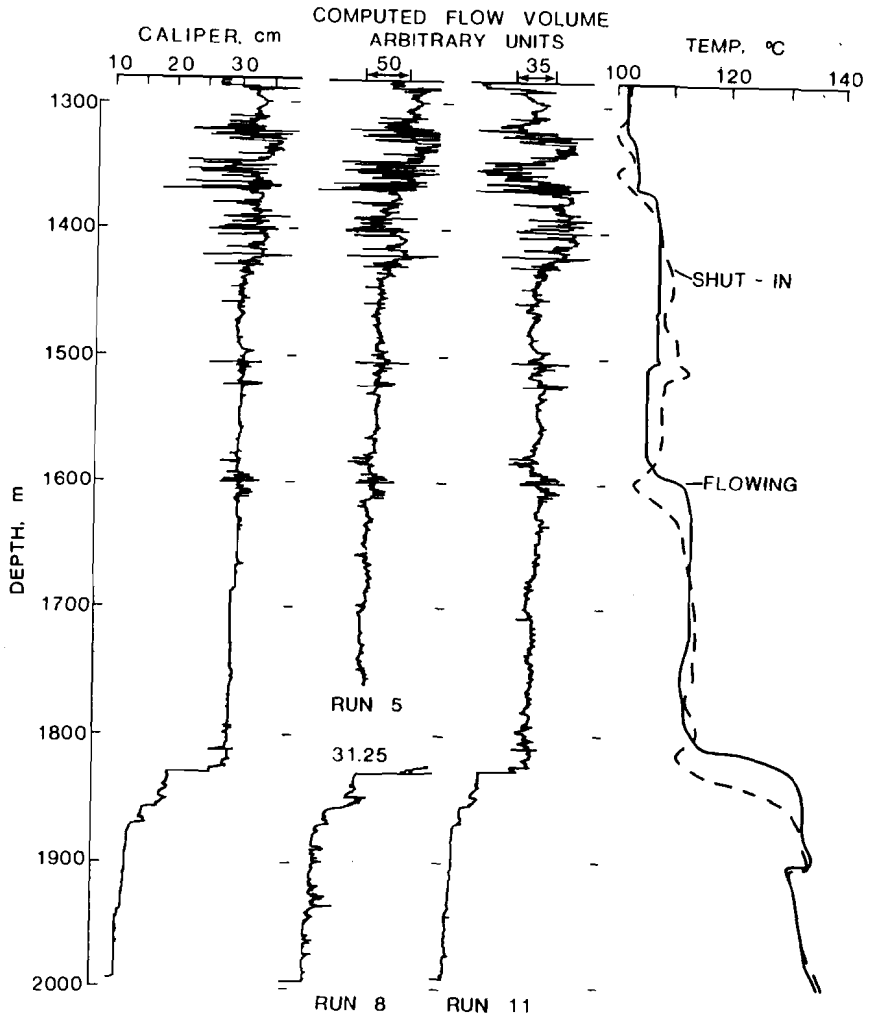

FIG. 17. Caliper, flow volume, and temperature logs of RRGE-2.

Substituting equation (3) into equation (4) with i equaling 1 and 2, and assuming the c_i is approximately the same, yields

$$\Sigma m_i / m_2 = -\Delta t_2 / \Delta t_i, \quad (5)$$

which can be used to estimate the ratio of the masses when the temperature changes are known.

Assuming that the fluids at a depth of 1755 m have been adiabatically mixed, the final temperature is 113.1°C; the initial temperature of the cold fluid is the shut-in minimum, 112.6°C at 1811 m, and the initial temperature of the hot fluid at 1890 m is 136°C (Figure 17). The adiabatic assumption may be violated by heat flowing from the borehole wall to the colder, mixed fluid, causing the apparent mixing temperature to be warmer than for adiabatic conditions. If this is the case, by applying equation (5) any inflow mass at greater depths would be less than or equal to 2.3 percent of the inflow at 1811 m.

At 1597 m, the temperature logs show a shut-in minimum and an inflection during flow. Flowmeter run 5 shows a higher volume of flow at 1554 m than at 1615 m. Again, this indicates that cold fluid flows in and up the borehole. A mixing temperature estimate, using equation (5), shows that the inflow at this depth is at least three or four times as large as the flow from the deeper zone.

The volume of flow at 1487 m on run 5 (Figure 17) is greater than the volume at 1524 m. The flow logs have many deflections between these two depths that may have been caused by turbulence; therefore, the exact depth of the inflow cannot be determined. At 1509 m, the shut-in temperature log shows a maximum of 113.6°C. The temperature log during flow shows an abrupt increase to 108°C at 1503 m, then remains constant for several hundred feet up the hole. This indicates an inflow of warmer fluid at 1503 m.

Flowmeter logs indicate that the volume of flow at 1311 m is considerably larger than the volume of flow at 1372 m. The shut-in temperature log shows two minima each of about 100°C, one at 1353 m, the other extending from 1327 m to 1317 m. The log recorded during flow shows a temperature decrease to 103.5°C at 1364 m and a drop to 102°C at 1323 m. Through this same depth range, flowmeter run 11 shows stalling and erratic behavior that could have been caused by turbulent inflow. These observations taken together imply that large volumes of colder fluid enter the hole at 1364 m and again at 1323 m.

After the USGS logged RRGE-2 several times during the period from March to July 1976, Idaho National Engineering Laboratory (INEL) made five temperature logs (Sandquist et al, 1976). These logs showed that the well warmed up but did not reach the temperature measured after drilling to the initial depth of 1829 m and before injection. On the last shut-in temperature log (INEL-4) the main temperature inversions remain prominent, showing that the fluid being produced is still colder than the surrounding formations. A temperature increase on the last log made during flow indicates that the warm influx at 1509 m is still active.

At the bottom of the casing, the flow logs showed a sharp break caused by the dependence of k on hole size. Run 5 indicates that the volume of flow in the casing was between 0.85 and 1.13 m³/minute. The flows calculated from differential pressure measurements across INEL's 85.7-mm orifice range from 1.48 m³/minute at startup to 1.34 m³/minute after flashing of water to steam had limited the flow.

In summary, the computed flow logs and two temperature logs provide a qualitative description of the various producing zones. There is little or no flow below 1811 m. The producing zone at 1597 m produced three or four times more fluid than the zone at 1811 m. When the well was shut in, this zone registered 104°C. Above that is a zone producing warmer fluid represented by the shut-in temperature of 113.6°C at 1509 m. Finally, two zones at 1364 m and at 1323 m, whose shut-in minimum is about 100°C, produce more than half the output of the well.

Fractures.—There is considerable evidence that most of the hot water entering both the deep wells and shallow holes in the Raft River reservoir is localized in fractures or fracture zones. The evidence is in three general, related categories: core showing numerous fractures; data suggesting depths of water entry such as temperature and flowmeter logs described above; and, most important, the caliper and acoustic televiewer logs showing the exact location and character of fractures producing hot water.

The USGS has made televiewer logs on parts of the following wells at Raft River: 23bb2, CH-3, CH-4, RRGE-2, RRGE-3, and RRGI-4. The earlier logs were made with a low-temperature televiewer tool while the logs of the deep wells were made with a high-temperature tool. Both tools experienced problems, chiefly with the magnetometer (part of the dip directions were either not available or questionable). However, some excellent logs were obtained where calculation of the angle of dip of bedding and fractures was possible. Data on bed orientation are

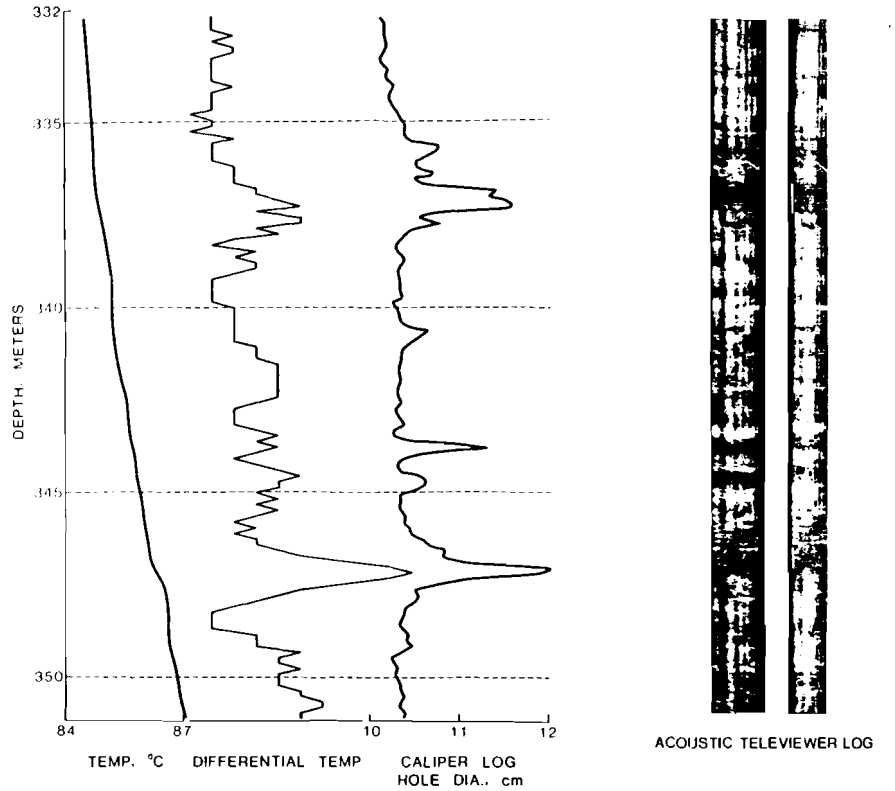

FIG. 18. Temperature log, computer-derived differential temperature log, caliper log, and two acoustic televiewer logs of CH-3.

described under structure. All directions are in respect to magnetic north. In each of the wells logged, there was some evidence that fractures seen on televiewer logs were producing most of the hot water flow.

The evidence for fracture sources is not as convincing in hole 23bb2 as in other holes (Figure 1). A temperature log made to the total depth of 98 m in 1974 indicated no major zones of inflow. When the well was deepened to 123 m, hot water flow within the well apparently increased (85–90°C). A temperature log made in 1976 after deepening suggested that there might be a zone at about 76 m that was accepting hot water from below. The televiewer and caliper logs show an open zone dipping 35 degrees that could be either bedding or a fracture. The rocks are less consolidated in this shallow hole than in the deeper holes so that acoustic reflections are lower amplitude and fractures are not as clearly defined. Nevertheless, it appears that there are fewer fractures in the shallower sediments in 23bb2 than in correlative sediments in CH-3.

Logs of CH-3 provide the best example of the relationship between flow and fractures. Figure 18 shows a composite of caliper, temperature, computer-derived differential temperature, and acoustic televiewer logs on the same detailed depth scale for the depth interval 332–351 m. Temperature logs of CH-3 indicate that most of the hot water flowing from the well enters the well in the depth interval 329–366 m. The caliper log of the well shows some anomalous borehole rugosity in the interval 335–347 m.

The differential temperature log in Figure 18 was calculated on the basis of a 0.61-m spacing. It is apparent that the greatest rate of temperature change at 347 m coincides exactly with the most significant anomaly on the caliper log. Another anomaly on the differential temperature log is within 0.3–0.6 m of another significant caliper deflection.

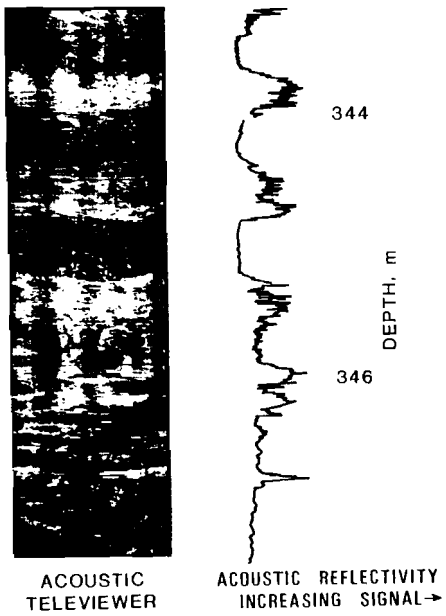

FIG. 19. Acoustic televiewer and acoustic reflectivity logs of CH-3.

Two televiewer logs were made of this section of the well at different times, and the results are almost identical (Figure 18). Major fracture zones occur at 337 m and at 347 m. The zone at 337 m is apparently the intersection of several fractures, all of which are steeply dipping and poorly defined. The lower, most open fracture strikes N85°W and dips approximately 70 degrees to the southwest. Just above the zone of open fractures are several closed fractures that may be cemented with silica. One of these dips to the northeast and one to the southeast; the dips are approximately 70 to 75 degrees. There are several clearly defined subparallel fractures at a depth of 334 m that dip 30 to 40 degrees to the east. These fractures appear to be less than 25 mm wide, and the adjacent rock does not appear brecciated as at 337 m. The temperature log indicates that the fractures at 334 m do not produce water. Descriptions of the core mention "many fractures" in the depth interval 338–353 m. Most of these fractures are filled or partly filled with silica or other noncalcareous material. The larger open fractures are not actually seen in the core because recovery was not complete, and the core that was recovered from those intervals is broken up.

At a depth of 344 m there is another caliper anomaly that is due to a soft bed between two hard beds. The rather uniform temperature gradient suggests that this soft bed does not produce water. There is one hard bed just above and two below the soft bed that are seen as white bands on the televiewer logs and as bit-sized intervals on the caliper log. The largest opening, and apparently the major source of hot water in CH-3, is at 347 m, just below the three hard beds. The rock at this depth appears to be somewhat brecciated on the televiewer log, and the fracture is poorly defined. Dip is apparently steep to the north. At a depth of 346 m, there is another tight fracture that dips about 50 degrees to the north.

The televiewer log does not answer the question of what localized the fracture zones that produce water. It does appear that the rocks in the altered zone from 302 to 354 m are somewhat more acoustically reflective than underlying rocks. This agrees with the observation that acoustic velocities are higher in the altered zone. Alteration has apparently produced a more competent rock. The underlying rocks appear more thin-bedded and shaly and thus may have yielded to stress by plastic flow and folding rather than fracturing.

The acoustic televiewer system was modified to enable the recording of an acoustic reflectivity log. It has been suggested that such a log might be related to porosity and permeability (Norel and Desbrandes, 1973). Figure 19 demonstrates the relationship of an acoustic televiewer log and an acoustic reflectivity log for the depth interval 343–347 m. The well cemented softer beds are clearly defined on the reflectivity log. The noisy intervals on the reflectivity log correspond to harder beds with a more irregular surface. The caliper log indicates that the drill hole was slightly larger through the beds with lower reflectivity. Hole diameter and actual reflectivity amplitudes cannot be distinguished without a separate caliper log. The caliper log shows the drill hole through the bed at 344 m to be approximately 9 mm larger than bit size and the hole through the bed at 345 m to be 3 mm larger than bit size. The main zone of hot water entry is at a depth of approximately

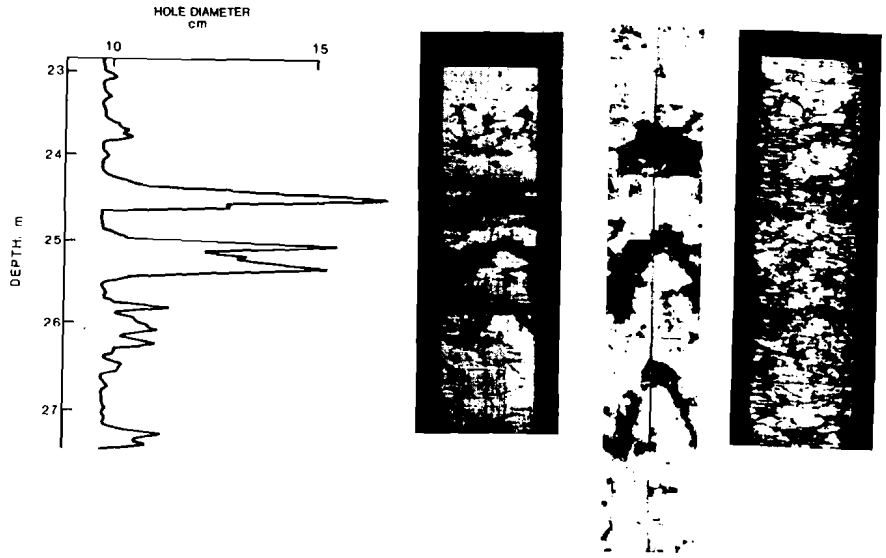

FIG. 20. Caliper log and three acoustic televiewer logs of CH-4.

47 m. Both the televiewer and reflectivity logs uggest the presence of thin, discontinuous hard ayers in this zone, which may represent silicification. his zone has a higher amplitude reflection, in spite f a larger hole diameter, than the beds at 344 and 45 m. Other high-resolution data are not available t this time. The acoustic reflectivity log would be seful to scan a hole at reasonably fast logging peeds to identify harder units that might display actures.

The televiewer logs of CH-4 (Figure 20) are of xcellent quality and very clearly show open fracures that are transmitting hot water. The temperature g of CH-4 shows a very rapid increase from the ater level at 4.3 m to a maximum temperature of 2°C at a depth of 18.3 m, which is the bottom of the sing. This temperature is maintained with little hange to a depth of 32.3 m, where the temperature gins a rapid decrease to a minimum of 31.5°C at e bottom of the hole. Almost all of the logs of this le suggest a change in lithology at a depth of 30 m. elow this depth, the total gamma radiation deases, apparent neutron porosity increases, and the mber and width of fractures decreases.

Figure 20 consists of three acoustic televiewer ns and a caliper log at the depth interval 23–27.5 m in CH-4. The character of open, water-transmitting fractures is shown very clearly. The fracture from 24.4 to 24.7 m is nearly horizontal. The fractures that bottom at 25.6 and 26.2 m dip 75 to 77 degrees in the direction N20°E. There is only one other large open fracture in the hole, at a depth of 28.6 m. There are a number of other well defined but tight fractures that dip 45 to 75 degrees northwest and northeast in the hole. A high-resolution caliper log of CH-4 shows that the borehole is at least 63.5 mm larger than bit diameter in the open fractures. The fractures are very irregular, probably because of solution by hot water moving through the openings. The most recent televiewer log of CH-4 indicates that some of these fractures are partly filled with very soft mud. The probe brought up some bentonitic drilling mud, but the source or mechanism for filling the fractures with mud is not known.

Composite interpretation of all of the logs of CH-4 suggests lateral movement of hot water through a system of fractures localized in a volcanic unit of the Salt Lake formation.

Prior to completion of this report it was possible to record acoustic televiewer logs of only short depth intervals of RRGE-2, and magnetic orientation was not obtained for all pictures; however, the logs do

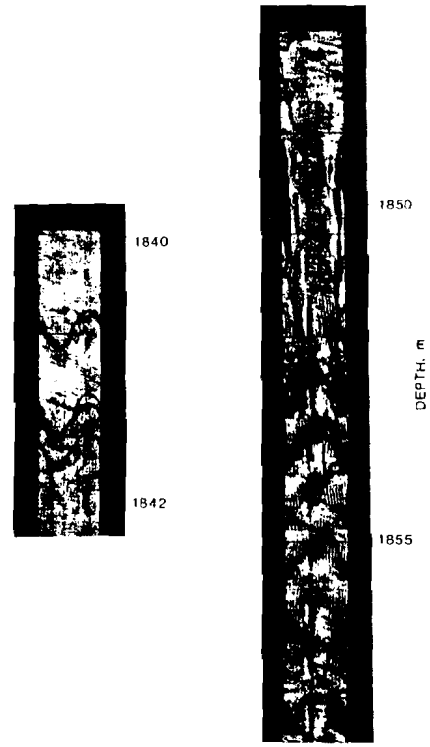

FIG. 21. Acoustic televiewer log of the depth intervals 1838–1842.5 m and 1847–1858 m, RRGE-2.

offer significant information. None of the fracture or bedding orientation data presented here are corrected for hole deviation, which in the RRGE wells is as much as 20.5 degrees from vertical. This will affect dip angle calculations significantly. A nearly vertical fracture system was recorded in the depth interval 1847–1857 m in RRGE-2 (Figure 21). The zone consists of two open fractures (faults?) that intersect the hole about 2.75 m apart vertically and another parallel fracture that intersects the well about 1.5 m higher. The vertical fracture is also intersected by several fractures of a parallel system, which was logged higher in the hole. These fractures, several of which are open, dip 35 to 50 degrees in the direction N15°E. Orientation was not measured directly on the vertical fracture system because of magnetometer failure; however, it is possible to derive evidence on the strike. If one assumes that the set of fractures dipping 35–50°E is the same in both the oriented and unoriented logs, then the strike of the nearly vertical fracture is approximately N85°E. The basis for this assumption of consistent orientation is quite sound because there are nine fractures in the depth interval 1829–1844 m with nearly the same orientation. The televiewer logs demonstrate a difference in acoustic reflectivity across the fracture zone, which suggests a change in lithology. This further substantiates the interpretation of the steep fracture zone as a fault.

In addition to the fractures shown on Figure 21, there are several poorly defined fractures below 1859 m in RRGE-2. One, at 1869–1871 m, dips approximately 76 degrees (strike unknown). Several fractures at 1871 m dip approximately 25 degrees. The televiewer log indicates another change in lithology across this fracture zone, which suggests that it may also be a fault. The log also indicates bedding between these two fractures. The layers dip between 18 degrees and 34 degrees. Drill-bit marks are common throughout the entire interval described, indicating that the rock is quite hard.

Despite the open fractures in hard rocks in RRGE-2, there is no direct evidence that hot water is being produced in significant quantities from any of the structures described above. Televiewer logs made at depths less than 1828 m are very poor quality because the hole was deviated or not circular in cross-section or both. A fracture zone of undetermined orientation was logged in the interval 1591.4–1597.1 m. This coincides with a major water-producing zone previously described and with fractures indicated on the caliper log. Another poorly defined open fracture at 1367 m is also a water-entry interval as indicated by temperature logs.

The deviation of leg C of RRGE-3 caused a problem with centralization of the televiewer and only logs of average quality were obtained (Figure 22). The dark vertical band on the logs in Figure 22 is due to the probe not being centered in the hole. Several fractures were clearly defined by both the televiewer and caliper logs. Anomalies on the USGS temperature log suggest that the fractures illustrated are contributing water to the hole. The upper fracture dips 6 degrees in the direction S70°W, and the lower fracture dips 34 degrees in the direction S75°E. Another water-producing fracture at a depth of 1490 m dips approximately 30 degrees in the direction S30°E. A commercial temperature log made in April 1977 confirms water entry just above 1554 m.

It appears that fractures are not as common in the deeper section of RRGE-3 as they are in RRGE-2. They could be hard to detect on the poorer quality logs; however, those mentioned are unmistakable on the televiewer logs and are also apparent on the caliper logs.

The acoustic televiewer log of RRGI-4 is very poor quality because of viscous mud in the hole and it is, therefore, impossible to identify any features related to water entry. However, a temperature log of RRGI-4, although made shortly after circulation of viscous drilling mud was completed, demonstrates changes in gradients that are probably due to the entry of hot water. The greatest changes occur in the interval 456–479 m; other changes in temperature gradient occur at the following approximate depths: 154, 182, 232, 350, and 396 m.

Distribution of radioisotopes

The distribution of naturally occurring radioisotopes is of considerable interest in geothermal exploration. It is of theoretical interest because of the relationship to radiogenic heat, but more practical applications are related to the identification of lithology and migration of radioisotopes in ground water. The distribution of uranium (U), thorium (Th), potassium (K), and their daughter nuclides provides more diagnostic information on lithology than the gross gamma intensity indicated by gamma logs. Furthermore, these isotopes may be selectively transported by ground water and particularly by hydrothermal solutions. Our data suggest that redistribution of naturally occurring radioisotopes by hydrothermal solutions has taken place in the Raft River reservoir.

U, Th, and K may be identified and the concentrations calculated from gamma spectra recorded in cased or open boreholes or wells. Continuous spectral logs can be recorded for energy windows that include major peaks representative of the concentrations of various radioisotopes. Such a log was run by a commercial service company on leg C of RRGE-3. A more accurate method is to select depths of interest from continuous logs and to record spectra with the probe stationary. The length of counting time is selected to reduce statistical error to an acceptable level. Figure 23 is an example of a spectrum recorded in CH-4. The quantity of radioisotope present is a function of the area under the peak after gain shift and spectral stripping programs have been run (Eggers, 1976).

The low-temperature gamma spectral probes used

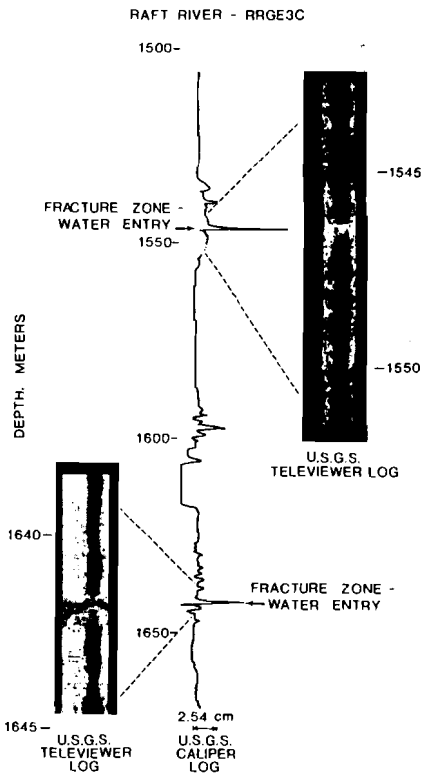

FIG. 22. Acoustic televiewer and caliper logs for the depth interval 1506–1670 m, RRGE-3, leg 3C.

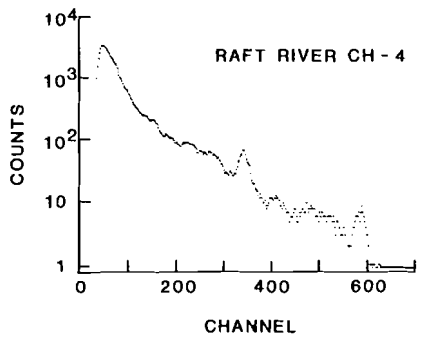

FIG. 23. Computer plot of gamma-ray energy spectrum at a depth of 42.9 m, CH-4.

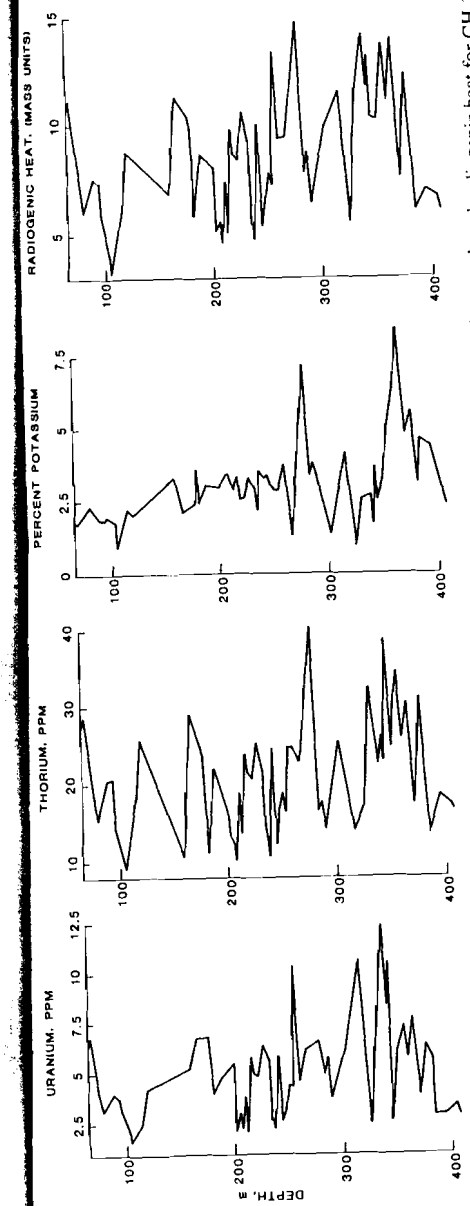

FIG. 24. Computer plot of laboratory radiometric analyses for radium equivalent uranium, thorium, potassium, and total radiogenic heat for CH-3.

in other areas by the USGS demonstrated excessive thermal drift. Laboratory radiometric analyses described in this report will provide the basis for calibration or in-hole spectra recorded at Raft River. Chemical analyses should also be performed to determine the equilibrium of the uranium decay series. Disequilibrium is certainly a possibility in a system where radioisotopes have been redistributed by hydrothermal solutions. Radon analyses should also be carried out in order to determine if radon creates a health hazard in the use of the water. Radon concentration also can be used to provide data on the origin of fluids and possibly to estimate reservoir porosity (Stoker and Krueger, 1975).

A detailed study of the distribution of U (radium equivalent), Th, and K (potassium 40 equivalent) was carried out in CH-3 and provides some basis for evaluating scattered analyses from other holes at Raft River. Figure 24 is a computer plot of the concentrations of U, Th, and K determined by radiometric analyses of core from CH-3. Although the distribution appears to be erratic, the plots suggest relationships of radioisotope concentration to the depths of hot water entry, 336.8 and 347.2 m, and hydrothermal alteration, 301.8–353.6 m. The highest U concentrations found in CH-3 were measured within the altered zone along with two of the lower concentrations. Th concentrations at a depth of 329–378 m are higher than average for the hole. Th concentration also tends to be highest in the finer-grained sediments with small pores and lowest in coarser-grained sediments with large pores. K content averages 1.87 percent (standard deviation $S = 0.36$) between 61 and 122 m, and 2.53 percent ($S = 1.05$) in the altered zone. The K content averages 3.55 percent ($S = 1.33$) for the rest of the hole with an apparent gradual increase with depth. The excellent correlation between potassium determined by spectral analysis and potassium feldspar suggests that spectral logging could be used to identify arkosic rocks.

Radiogenic heat was calculated from the radiometric analysis (Figure 24). The radiogenic heat is somewhat higher than average in the deeper part of the altered zone. Plots of radiogenic heat versus porosity indicate a general tendency toward higher porosity in the more radioactive rocks. Pore-size distribution studies, however, suggest that these rocks are likely finer grained and the permeability lower than rocks with lower porosity. Radiometric ratios are somewhat easier to obtain from borehole data and may be more indicative of major changes in the system than absolute quantities. Figure 25 shows

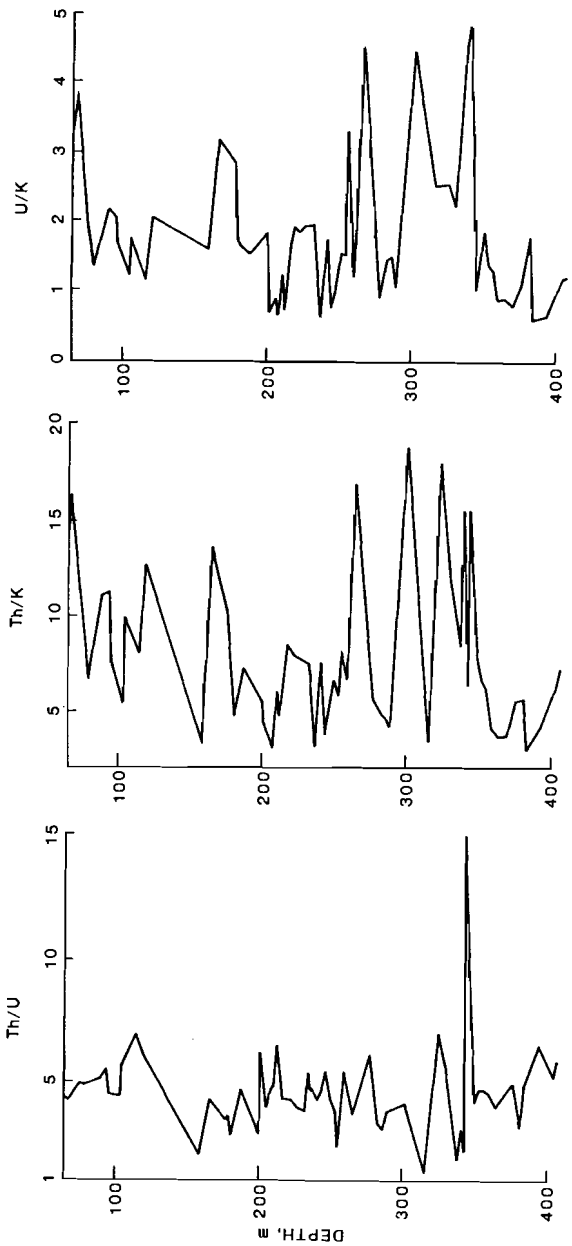

FIG. 25. Computer plot of thorium/uranium, thorium/potassium, and uranium/potassium ratios, CH-3.

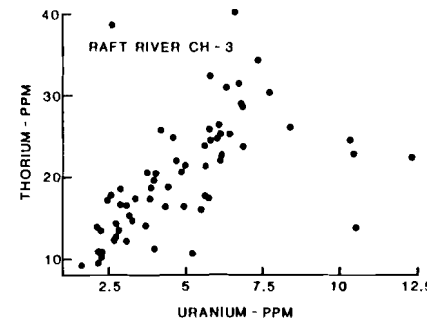

FIG. 26. Plot of thorium versus uranium, CH-3.

depth plots of the Th/U, Th/K, and U/K ratios for CH-3. The Th/U plot shows a very significant anomaly at 345 m, which is within 2.5 m of the major zone of hot water entry. The Th/K plot is erratic, but the highest ratios are in the altered zone. The U/K plot shows an interval of higher values in the altered zone. Crossplots of the radiometric values show no significant relationships, except for Th versus U which has a linear relationship at concentrations less than 27 parts per million (ppm) Th, 7 ppm U, and considerable scatter at higher concentrations (Figure 26). The correlation coefficient (γ) for all Th and U analyses in CH-3 is 0.49; for samples less than 27 ppm Th and 7 ppm U, it is 0.77 (number of samples, $n = 51$). The γ for Th and U in all samples from other Raft River boreholes is 0.80, except for the andesite in CH-4 where it is -0.64 ($n = 10$). It is interesting to note that the γ is -0.82 ($n = 12$) for the Th and U analyses in CH-3 that exceed 27 ppm and 7 ppm, respectively. The data are not sufficient to conclude that a negative γ for Th and U signifies hydrothermal alteration or is characteristic of andesite in the Raft River area.

The Th content in the andesite has a mean value of 27.82 ppm ($S = 1.64$). This very uniform concentration suggests little redistribution by hot water moving through the andesite. In contrast, the mean for U is 5.82 ppm ($S = 1.78$). It is likely that the original U concentration was uniform in the andesite flow, and it has been redistributed by hot water. Almost all concentrations of Th greater than 27 ppm, and of U greater than 7 ppm, are found in and immediately adjacent to the altered zone in CH-3. Figure 25 demonstrates that both the highest and lowest Th/U ratios are found in this zone. All evidence suggests redistribution of U and Th by the hydrothermal solution that altered the rocks. Thus, it appears that gamma spectral logging and field calculation of radiometric ratios would be useful for identifying hydrothermally altered zones that are potential sources of hot water.

Considering the genesis of the radioelement anomaly in CH-3, it seems more likely that U would be transported in hot ground water than would Th because the former is considerably more soluble in most ground water than is Th. The negative γ in CH-4 and the altered zone in CH-3 are difficult to explain, but the samples are too few to justify any conclusions at this time.

Six core samples from the depth interval 1372–1388 m in RRGE-1 were analyzed radiometrically. The geophysical logs suggest that this rock, which is immediately above the schist, is considerably different from most of the overlying Salt Lake formation. The mean contents of U, Th, and K are 6.45 ppm, 27.27 ppm, and 3.50 percent, respectively. The γ for U and Th is 0.76. The only thing anomalous about the radioisotope distribution in these few deep samples is a Th concentration of 43 ppm and two K concentrations of 5 and 6.5 percent. The only analyses from elsewhere in Raft River that show such high concentrations are from the altered zone in CH-3.

Just prior to the completion of this report, a continuous spectral log was run commercially on RRGE-3, leg C. Unfortunately, quantitative interpretation of this log was ruled out by the absence of corrections for hole diameter and for cased, cemented, or open-hole conditions. Moreover, the log indicates numerous zero and negative concentrations for K and U, implying that stripping ratios used to calculate these concentrations were incorrect. Th concentrations indicated by this log may be more reliable, although the Th curve ranges between 0 and 15 ppm in the depth interval from 2.4 to 436 m, which does not agree with our data from CH-3 (Figure 24). The Th curve ranges from 0 to 25 ppm in the interval from 436 to 1292 m, which are more reasonable values. From 1292 to 1716 m, Th concentrations up to 60 ppm were recorded; from 1716 m to total depth, Th concentrations up to 140 ppm were recorded. From 1769 to 1798 m, U concentrations up to 110 ppm were recorded. We have no sample results to corroborate the high Th and U concentrations; however, a relationship between logs made by two different companies in RRGE-1 and RRGE-3 suggests that these concentrations are of the correct order of magnitude. The Th maxima are more likely correct

than the U maxima, which are probably too high.

Comparison of computed and measured water resistivities

The resistivity of the formation fluid R_{wc} can be calculated from resistivity and porosity logs by Archie's equation in some cases (Keys and MacCary, 1971). In this report the symbol R_{wc} is used for the calculated water resistivity to distinguish it from R_w, the resistivity actually measured on a sample of fluid from the borehole. Archie's equation is

$$R_{wc} = R_t/F = aR_t\phi^{-m}, \qquad (6)$$

where a and m are empirically determined parameters, and the formation resistivity R_t is taken from the deepest-investigating resistivity log available for each hole. The formation resistivity factor F was measured on a few core samples from CH-3, but for most calculations it is assumed to be equal to the reciprocal of the square of the porosity. The parameter a is assumed to be unity. The porosity ϕ is derived from the neutron log or gamma-gamma log for RRGE-1 and from laboratory measurement of effective porosity for CH-3. R_w values were corrected to borehole temperatures. The values calculated using these data are given in Table 4.

All the R_{wc} values calculated for CH-3 are higher than the R_w values. Calculations were made at depths of probable hot water entry zones as indicated by the logs. Within each zone selected, a depth with a minimum resistivity was chosen. The second R_{wc} value given for depth 370 m was calculated using the laboratory-measured formation factor of the nearest core sample that had similar effective porosity.

A calculation of interstitial fluid resistivity in RRGE-2 was made at a depth of 1465 m, the depth to which the hole had been drilled when the water samples for analysis were collected. The depths for two shallower calculations were depths of inflow determined previously. At each depth R_{wc} was less than R_w. This could be due to the electrical conductivity of fluids in fractures. Electrolyte filling the volume of a fracture provides a less resistive path than an equal volume of electrolyte filling ill-connected, interstitial porosity. The neutron and gamma-gamma logs are related to the total volume of porosity and do not distinguish fractures from pores; therefore, in fracture conduction the ϕ in equation (6) will remain the same while R_t is lower.

In summary, it is unlikely that correct R_w values can be derived from R_{wc} calculations without empirical control.

CONCLUSIONS AND RECOMMENDATIONS

The study described is only preliminary but serves to illustrate the advantages and limitations of borehole geophysical measurements in exploration and development of a geothermal reservoir. The effectiveness of such a program can be greatly improved by planning and coordinating surface surveys, drilling, coring, casing, well logging, and laboratory analyses.

At Raft River, more data are needed to develop an adequate description of the reservoir, particularly the deeper part. Specifically needed are more core and laboratory analyses and much more open-hole logging under both flowing and shut-in conditions. Logging equipment for use in such high-temperature environments requires improvement in reliability of operation and accuracy. Furthermore, quality control of well logs is essential in these novel environments where logging experience is lacking. Finally, much more research is needed to develop viable log interpretation and calibration methods for geothermal reservoir rocks. In our opinion, this can best be accomplished by using the computer to establish relationships between different types of logs and between logs and core and hydrologic test data. For these purposes there must be enough laboratory analyses and test data to be statistically significant, and these data should be selected on the basis of log response.

Table 4. A comparison of fluid resistivities calculated from logs and measured on water samples.

Well no.	Depth (m)	ϕ (percent)	R_t (Ω-m)	R_{wc} (Ω-m)	R_w (Ω-m)
RRGE-2	1317	15	10	0.22	
	1365.5	18–27	10	0.32–0.73	1.1
	1465.5	3	400	0.36	
CH-3	370	41	7.5	1.26	
	370	—	—	1.35	0.6–0.9
Sample 74	330.4	46	7.5	1.59	

ACKNOWLEDGMENTS

An interactive crossplot computer program was written by D. R. Posson of the USGS. D. E. Eggers and T. A. Taylor of the USGS Borehole Geophysics Project wrote several computer programs described in this report. T. A. Taylor generated several hundred plots from which the few included here were selected. Personnel of the Idaho National Engineering Laboratory, in particular R. C. Stoker, were helpful in providing access to wells and data.

REFERENCES

Burke, J. A., Schmidt, A. W., and Campbell, R. L., Jr., 1969, The litho-porosity cross plot: Log Analyst, no. 6, p. 25–43.

Campbell, A. S., and Fyfe, W. S., 1965, Analcime-Albite equilibria: Am. J. Sci., v. 263, p. 807–816.

Coombs, D. S., Ellis, A. J., Fyfe, W., and Taylor, A. M., 1959, The zeolite facies with comments on the interpretation of hydrothermal synthesis: Geochim. et Cosmochim. Acta, v. 17, p. 53–107.

Crosthwaite, E., G., 1976, Basic data from five core holes in the Raft River geothermal area, Cassia County, Idaho: U.S.G.S. open file rep. 76-665, p. 12.

Eggers, D. E., 1976, The application of borehole geophysics to the selection and monitoring of nuclear waste disposal sites: proc. 17th U.S. sympos. of rock mechanics, Snowbird, Utah, B3-1-4 B3-7, p. 4.

Goodwin, L. J., Haigler, L. B., Rioxs, R. L., White, D. E., Muffler, L. J. P., and Wayland, R. G., 1971, Classification of public lands valuable for geothermal steam and associated geothermal resources: U.S.G.S. circ. 647, p. 1–18.

Keys, W. S., and MacCary, L. M. 1971, Application of borehole geophysics to water resources investigations: U.S.G.S. Techniques Water Resources Inv., Book 2, Chap. E1, 124 p.

Kunze, J. F., Stoker, R. C., and Goldman, D., 1977, Heat transfer in formation as a geothermal reservoir engineering tool: ASME, Heat Trans. Div., 77-HT-88, 8 p.

Norel, G., and Desbrandes, R., 1973, Une nouvelle diagraphie des sondages par reflexion ultra sonique: Revue De' E' Institut Francais Du Petrole, v. 28, no. 4, p. 587–604.

Sandquist, G. M., Swanson, S. R., Stoker, R. C., and Kunze, J. F., 1976, On evaluating the energy capacity and lifetime of fracture dominated geothermal reservoirs: proc., 12th Intersociety Energy Conversion Eng. Conf., Washington, D. C., 6 p.

Stoker, A. K., and Krueger, Paul, 1975, Radon measurements in geothermal systems: Stanford Univ., SGP-TR, p. 11–116.